frontiers | Frontiers in Electronic Materials

ORIGINAL RESEARCH
published: 08 June 2022
doi: 10.3389/femat.2022.892496

Coevolution of Superconductivity With Structure and Hall Coefficient in Pressurized $NaSn_2As_2$

*Jing Guo[1,2], Cheng Huang[1,3], Sijin Long[1,3], Yazhou Zhou[1], Shu Cai[1], Xiaodong Li[4], Yanchun Li[4], Ke Yang[5], Aiguo Li[5], Jiangang Guo[1], Qi Wu[1] and Liling Sun[1,2,3]**

[1]Institute of Physics, Chinese Academy of Sciences, Beijing, China, [2]Songshan Lake Materials Laboratory, Dongguan, China, [3]University of Chinese Academy of Sciences, Beijing, China, [4]Institute of High Energy Physics, Chinese Academy of Sciences, Beijing, China, [5]Shanghai Synchrotron Radiation Facilities, Shanghai Institute of Applied Physics, Chinese Academy of Sciences, Shanghai, China

A new class of van der Waals-type layered materials, ASn_2Pn_2 (A= Li, Na, Sr, Eu; Pn= As, P, Sb), has attracted much attention in the field of condensed matter physics because they have interesting physical properties and various ground states, as well as potential applications. Here, we are the first to report the close connection among the superconducting transition temperature T_c, crystal structure and Hall coefficient in pressurized $NaSn_2As_2$ single crystal. We found that the superconducting $NaSn_2As_2$ displays two pressure-induced crystal structure phase transitions, first from an ambient-pressure rhombohedral (R) phase to a monoclinic (M) phase starting at ~ 12 GPa (P_{C1}), and then to a simple cubic (C) phase starting at ~ 33 GPa (P_{C2}). In these phases, the T_c value and carrier concentration change correspondingly. Our results suggest that the observed three superconducting states are related to the change of structural phase and the variation of carrier concentrations.

Keywords: superconductivity, structure phase transition, Hall, high pressure, NaSn2As2

Edited by:
Yihua Wang, Fudan University, China

Reviewed by:
John Tranquada, Brookhaven National Laboratory (DOE), United States
Yosuke Goto, National Institute of Advanced Industrial Science and Technology (AIST), Japan

****Correspondence:***
Liling Sun
llsun@iphy.ac.cn

Specialty section:
This article was submitted to Superconducting Materials, a section of the journal Frontiers in Electronic Materials

Received: *09 March 2022*
Accepted: *18 May 2022*
Published: *08 June 2022*

Citation:
Guo J, Huang C, Long S, Zhou Y, Cai S, Li X, Li Y, Yang K, Li A, Guo J, Wu Q and Sun L (2022) Coevolution of Superconductivity With Structure and Hall Coefficient in Pressurized $NaSn_2As_2$. Front. Electron. Mater. 2:892496. doi: 10.3389/femat.2022.892496

INTRODUCTION

The new class of van der Waals-type layered materials ASn_2Pn_2 (A= Li, Na, Sr, Eu; Pn= As, P, Sb) exhibits special physical properties and different ground states, such as low thermal conductivity (Lee et al., 2015; Lin et al., 2017), topological state (Rong et al., 2017; Gui et al., 2019), magnetically topological insulating state (Gibson et al., 2015; Li et al., 2019) and superconducting state (Goto et al., 2017; Cheng et al., 2018; Goto et al., 2018; Ishihara et al., 2018; Yuwen et al., 2019; Zhao et al., 2021), etc. Since ASn_2Pn_2 has a layered structure, similar to cuprate and iron-based superconductors (Bednorz and Muller, 1986; Wu et al., 1987; Hsu et al., 2008; Kamihara et al., 2008; Guo et al., 2010; Wang et al., 2011; Chu et al., 2015; Arguilla et al., 2016; Hu, 2016; Goto et al., 2018; He et al., 2019; Proust and Taillefer, 2019), it is expected that the materials may present superconductivity or emerge exotic phenomena through chemical doping or applied pressure. Earlier studies on $Na_{1+x}Sn_{2-x}As_2$ and $Na_{1-x}Sn_2P_2$ found that the superconductivity can be truly developed by Na doping on the Sn site or self-doping by Na vacancy defects (Goto et al., 2018; Yuwen et al., 2019), indicating that the superconductivity of these materials is sensitive to the tuning parameters.

Pressure is an effective method to tune crystal and electronic structure without changing chemistry. Which can be used as a probe to test whether there is a link between the crystal structure and superconductivity in van der Waals-type layered materials. In this paper, we are the first to report the connection among the crystal structure, Hall coefficient (R_H) and T_c in the

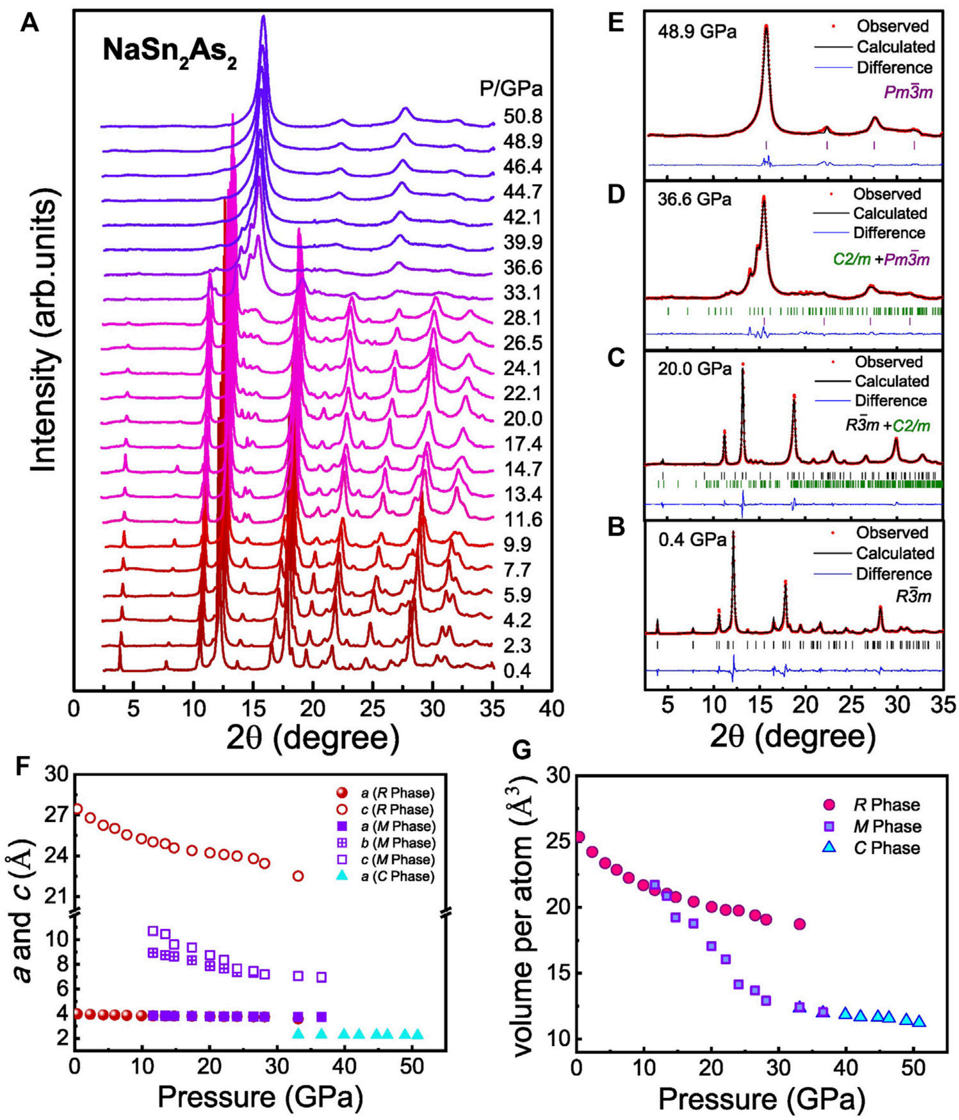

FIGURE 1 | Structure information of $NaSn_2As_2$ under high pressure. **(A)** Powder X-ray diffraction patterns collected at different pressures, showing two structure phase transitions that occur at ~ 11.6 and ~ 33.1 GPa, respectively. In the experiments, a monochromatic X-ray beam with a wavelength of 0.6199 Å was employed **(B–E)** Analysis of the XRD patterns measured at 0.4, 20.0, 36.6 and 48.9 GPa, showing that the $NaSn_2As_2$ sample evolves from a rhombohedral phase ($R\bar{3}m$) to a monoclinic (*C2/m*) phase, and then to a simple cubic phase **(F–G)** Pressure dependence of the lattice constants and atomic volume (*V*) in the rhombohedral (*R*), monoclinic (*M*), and cubic (*C*) phases.

superconducting $NaSn_2As_2$, through the complementary measurements of *in-situ* high-pressure X-ray diffraction (XRD), electric resistance, *ac* susceptibility and Hall coefficient.

The high-quality single crystal samples were synthesized by solid-state reaction methods, as reported elsewhere (Lin et al., 2017). High pressure was generated by a Diamond anvil cell (DAC) with two opposing anvils sitting on the Be-Cu supporting plates. In the high-pressure measurements, diamond anvils with 300 μm flats were employed to create pressure, and NaCl powder was adopted as pressure transmitting medium. High pressure resistance and Hall coefficient measurements were carried out using four-probe technique and Van der Paw method (van der Pauw, 1958), respectively. High-pressure alternating-current (*ac*) susceptibility measurements were performed by using the home-made primary/secondary-compensated coils around the diamond anvil (Debessai et al., 2008; Sun et al., 2012). High pressure x-ray diffraction (XRD) measurements were carried out at beamline 4W2 at Beijing Synchrotron Radiation Facility and at beamline 15U at the Shanghai Synchrotron Radiation Facility, respectively. The polycrystalline samples prepared for the x-ray diffraction measurements were obtained

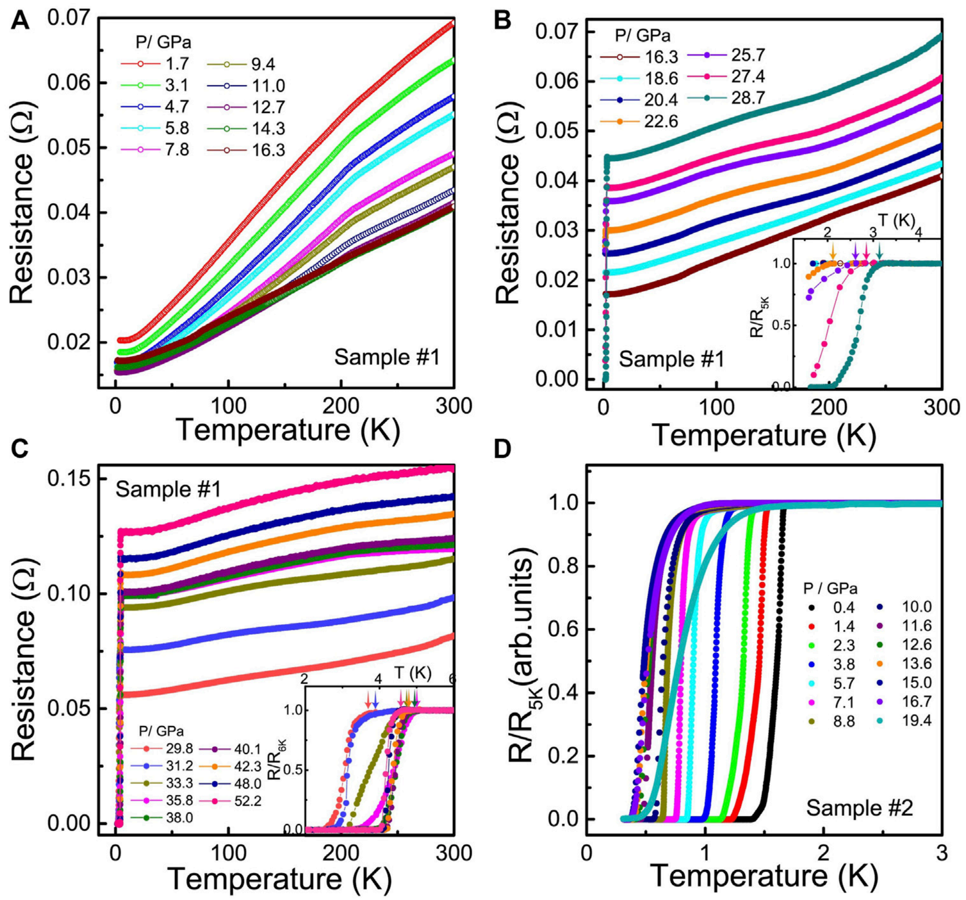

FIGURE 2 | Electrical resistance (*R*) as a function of temperature (*T*) at different pressures. **(A–C)** For the sample #1 measured down to 1.5 K, insets in **(B)** and **(C)** display the enlarged views of the normalized *R-T* curves in the lower temperature range. **(D)** Normalized *R-T* curves measured down to 0.3 K for the sample #2, exhibiting superconducting transition with zero resistance in the pressure range of 0.4–19.4 GPa.

by grinding single-crystal samples. The pressure in all experiments was determined by the ruby fluorescence method (Mao et al., 1986).

We first performed *in-situ* high pressure XRD measurements. **Figure 1A** shows the XRD diffraction patterns collected at different pressures up to ~ 50 GPa. It is found that all patterns below 9.9 GPa can be indexed well by the rhombohedral (*R*) phase with space group $R\ \bar{3}\ m$ (**Figure 1B**), as what was observed at ambient pressure (Lin et al., 2017). However, new peaks appear when pressure is increased up to 11.6 GPa, indicating that application of pressure induces the structure change. The analysis on the XRD patterns for this high-pressure phase reveals that the sample partially transforms into the monoclinic (*M*) phase (*C2/m*) (**Figure 1C**). The two coexisted phases (*R* and *M*) persist up to ~ 30 GPa before another obvious change of the XRD patterns at ~ 33 GPa (**Figure 1D**), where the presence of a new sets of diffraction peaks suggests that pressure drives a new phase transition. We found that the new phase can be indexed to a simple cubic phase (**Figure 1E**). The refinements of the XRD results allow us to obtain the pressure dependence of lattice parameters and corresponding volume for the *R*, *M* and *C* phases (**Figures 1F,G**).

$NaSn_2As_2$ crystalizes in rhombohedral (*R*) unit cell at ambient pressure, similar to that of Bi_2Te_3 or Bi_2Te_2Se (Kushwaha et al., 2016). Theoretical calculations indicate that Bi_2Te_3 undergoes structural phase transitions under pressure, from *R* phase to *M* phase, and eventually to *C* phase due to that the *C* phase has a lower enthalpy (Zhu et al., 2011). Our high pressure XRD measurements reveal that $NaSn_2As_2$ shows the similar high-pressure behavior as Bi_2Te_3, occurring the transitions of *R*-to-*M*-to-*C* phase upon increasing pressure. The same phase evolution observed in our compressed $NaSn_2As_2$ sample allows us to propose that these two materials may share the same mechanism of driving the phase transition.

To investigate the pressure effects on the transport properties of $NaSn_2As_2$ in these different phases, we carried out *in-situ* high pressure resistance measurements for the sample. **Figures 2A–C** show the electrical resistance as a function of temperature under different pressures up to 52.2 GPa for the sample #1. Below 12 GPa, a tiny kink is observed at around 200 K, which has also been found by Pugliese et al. (2019). We propose that this

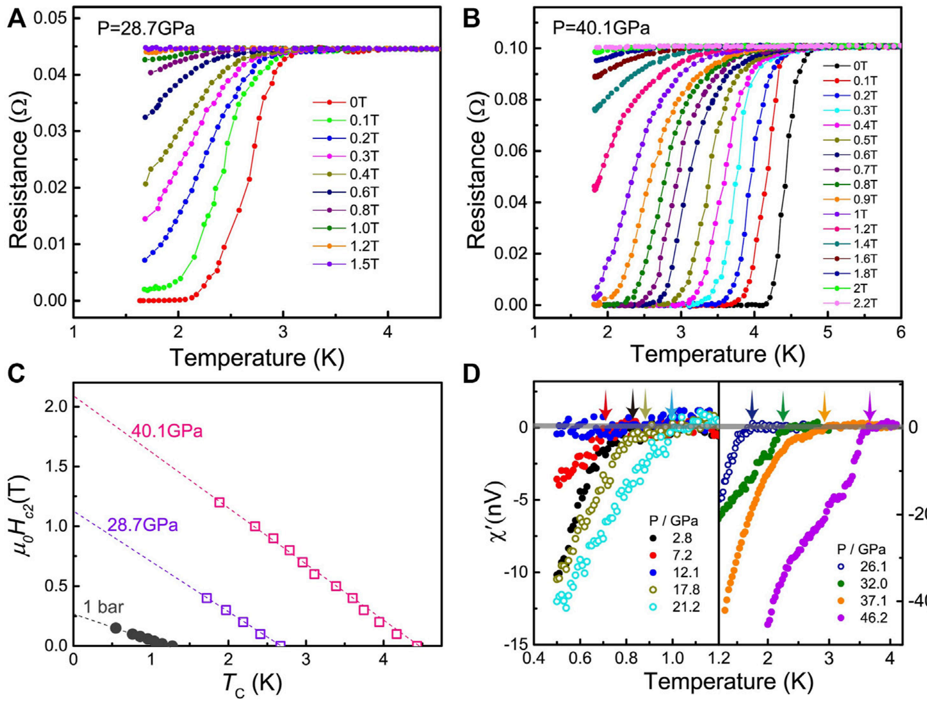

FIGURE 3 | Characterization of superconducting transitions in pressurized $NaSn_2As_2$. **(A–B)** Temperature dependence of electrical resistance under different magnetic fields at 28.7 and 40.1 GPa, respectively. **(C)** Estimations of superconducting upper critical field (H_{c2}) as a function of superconducting transition temperature (T_c) at ambient pressure (Goto et al., 2017), 28.7 and 40.1 GPa, the dashed lines represent the slopes of the estimated upper critical fields $(dH_{c2}/dT)_{T=Tc}$ at different pressures. **(D)** The real part of the alternating-current susceptibility (χ ′) as a function of temperature at different pressures. The arrows indicate the onset temperatures of superconducting transitions.

anomaly may be associated with an instability of the CDW order. Since the ambient-pressure superconducting transition of $NaSn_2As_2$ is about 1.3°K (Goto et al., 2017; Cheng et al., 2018; Ishihara et al., 2018), which is lower than the base temperature (1.5 K) of the cryostat employed for this run, no resistance drop is observed. However, we find that the normal resistance value versus temperature is reduced with increasing pressure up to 12.7 GPa, then it is enhanced with further compression, we propose that the observed phenomenon should be attributed to the partial *R-M* phase transition (**Figures 2A,B**).

Noticeably, a resistance drop is found at ~2.1 K at 22.6 GPa (as shown in the inset of **Figure 2B**) and it shifts to higher temperature with further compression. A zero-resistance state is observed at 1.5 K at 28.7 GPa and above, indicative of an emergence of a superconducting transition (inset of **Figure 2B** and **Figure 2C**). The transition temperature (T_c) is enhanced upon increasing pressure and remains almost unchanged at pressure higher than ~ 36 GPa (**Figure 2C**). To understand the full evolution process of T_c with pressure at lower temperature for $NaSn_2As_2$, we performed high-pressure resistance measurements for the sample #2 in another cryostat that can cool the sample down to ~ 0.3 K (**Figure 2D**). We observed a superconducting transition at 1.4 K at the lowest pressure of 0.4 GPa, adopted in this study, close to the T_c obtained at ambient pressure (Goto et al., 2017; Cheng et al., 2018; Ishihara et al., 2018). With increasing pressure, T_c decreases down to ~ 0.3 K at ~ 13 GPa and then increases with further compression up to 19.4 GPa (**Figure 2D**).

To support the observed resistance drops in pressurized $NaSn_2As_2$ are attributed to superconducting transitions, we performed resistance measurements under different magnetic fields for the sample subjected to 28.7 and 40.1 GPa (**Figure 3A** and **Figure 3B**). It is found that the resistance drops shift to lower temperature with increasing magnetic field (**Figure 3A** and **Figure 3B**). We also performed alternating-current (*ac*) susceptibility measurements on the sample in the pressure range of 2.8–46.2 GPa and found the diamagnetism (**Figure 3C**). The evolution of T_c with pressure obtained from the *ac* susceptibility measurement is consistent with that measured by the resistance. These results confirm that the pressure-induced resistance drop originates from the superconducting transition. We extract midpoint T_c as a function of magnetic field and estimate the value of the upper critical magnetic field (H_{c2}) at zero temperature by Werthamer-Helfand-Honhenberg (WHH) formula ($H_{c2}^{WHH}(0)$ = $-0.693T_C(dH_{c2}/dT)_{T=Tc.}$) (Werthamer et al., 1966). The H_{c2} value is ~ 1.2 T at 28.7 GPa and ~ 2.1 T at 40.1 GPa (**Figure 3D**), which are much higher than the value of ~ 0.25 T obtained at ambient pressure (Goto et al., 2017). These results indicate that the three superconducting phases are different in nature.

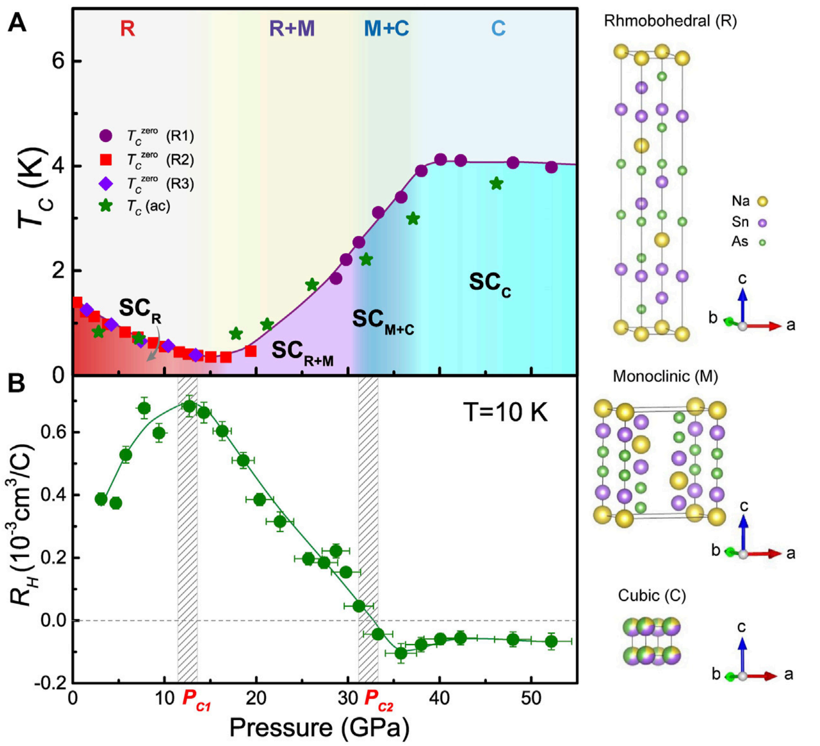

FIGURE 4 | Pressure-temperature phase diagram combined with structural phase information and Hall coefficient of $NaSn_2As_2$. **(A)** Pressure-T_c phase diagram with structural information. T_c^{zero} (R) stands for the zero-resistance temperature of superconducting transition obtained from resistance measurements. T_c (*ac*) represents the superconducting transition temperature measured through *ac* susceptibility measurements. SC_R, SC_{R+M}, SC_{M+C} and SC_C represent superconducting phases in the rhombohedral phase, mixed rhombohedral and monoclinic phases, mixed monoclinic and cubic phases and single cubic phase, respectively. **(B)** Hall coefficient (R_H) as a function of pressure measured at 10 K. P_{C1} and P_{C2} stand for the critical pressures of structural phase transition, respectively.

We summarized the pressure dependence of superconducting transition temperature T_c and structure information in **Figure 4A**. To compare $T_c(P)$ detected from resistance and *ac* susceptibility measurements in a unified way, we used zero-resistance T_c in the phase diagram. It is seen that T_c of the ambient-pressure superconducting phase decreases continuously with increasing pressure up to P_{C1} (~ 12 GPa), where the *R* phase partially transforms to the *M* phase. Meanwhile, the T_c increases with further compression up to ~ 31 GPa. By applying higher pressure, the simple cubic phase appears and coexists with the *M* phase, in which T_c rises in this pressure range. When pressure is higher than 36 GPa, the structure transforms into a pure single cubic phase and the corresponding T_c remains almost unchanged. These results show that the T_c are strongly influenced by the structural phase transition. To further understand the change of superconducting transition temperature in pressurized $NaSn_2As_2$, we performed high-pressure Hall coefficient measurements on the sample by sweeping the magnetic field perpendicular to the *ab* plane up to 2 T at 10 K. The pressure dependence of Hall coefficient (R_H) is illustrated in **Figure 4B**. It is found that R_H is positive in the *R* phase, reflecting the dominance of hole carriers (the carriers in the studied material are composed of hole and electron carriers). Meanwhile, the value of R_H is enhanced with elevating pressure and reaches a maximum at ~ P_{C1}, implying that the role of the hole carrier is reduced with increasing pressure and it may be responsible for the monotonic decline of T_c in this pressure range. In the pressure range of a coexistence of *R* and *M* phase (12–31 GPa), R_H is still positive but decreases dramatically with increasing pressure, suggesting that the role of hole carriers is weakened by applying pressure. It suggests that the structural phase transition enhances the contribution of electron carriers which seems to be in favor of superconductivity. It is worth noting that the tendency of the change in $T_c(P)$ is contrary to that in $R_H(P)$ in the superconducting phase with the dominance of hole carriers (**Figures 4A,B**), implying that the component of the carriers plays a vital role in determining T_c of this material. At pressure about 33 GPa (P_{C2}), R_H goes through zero, suggesting that both holes and electrons are likely present and making compensating contributions. At $P>$ P_{C2}, the cubic phase appears and R_H changes its sign from positive to negative, demonstrating that the *M*-to-*C* phase transition gives rise to a drastic change in the character of the first Brillouin zone, which impacts directly on the T_c value, and the cubic superconducting phase with the domination of electron carriers holds highest T_c (~ 4.1˚K). Noted that $NaSn_2As_2$ exhibit opposite conduction polarities along in-plane and cross-plane directions due to the unique Fermi surface geometry (He et al., 2019). The Hall coefficient shown in this study is obtained from the in-plane measurement, how the cross-plane Hall coefficient changes with pressure deserves further investigations in the future.

In conclusion, we have investigated high-pressure coevolution of superconductivity with structure and transport properties for $NaSn_2As_2$, one of the van der Waals-type layered materials, through *in-situ* measurements of XRD, resistance, *ac* susceptibility and Hall coefficient. We found a close correlation of superconductivity with crystal structure and Hall coefficient. Based on the evolution from the ambient-pressure superconducting phase of $NaSn_2As_2$, we find that pressure induces two dramatic changes of superconductivity that are associated with the *R-M* phase at the critical pressure of 12 GPa (P_{C1}) and *M-C* phase transition at another critical pressure of ~ 33 GPa (P_{C2}), respectively. Hall coefficient measurements find that the tendency of the change in $T_c(P)$ of the rhombohedral and monoclinic superconducting phases is opposite to that in $R_H(P)$, suggesting that hole carriers are dominant in these SC phases, At P_{C2}, the Hall coefficient change the sign from positive to negative, meanwhile the sample undergoes a structure phase transition from the *M* phase to the *C* phase. The T_c value of the cubic phase is higher than that of the rhombohedral and monoclinic superconducting phases. The connection among the superconductivity, structural phase transition and R_H revealed by our high-pressure study is expected to shed new insight on the underlying superconducting mechanism of the tin-pnictide-based superconductors and provide a route to explore new superconductors with potential applications.

DATA AVAILABILITY STATEMENT

The original contributions presented in the study are included in the article/Supplementary Material, further inquiries can be directed to the corresponding author.

AUTHOR CONTRIBUTIONS

LS designed the study and supervised the project. JGG grew the single crystals. JG, CH, SL, YZ, SC and LS performed the high pressure resistance, ac susceptibility and Hall measurements. JG, YL, XL, KY and AL performed the high-pressure X-ray diffraction measurements. LS, JG and QW wrote the manuscript in consultation with all authors.

FUNDING

This work in China was supported by the NSF of China (Grant Numbers Grants No. 12122414, U2032214, 12104487 and 12004419), the National Key Research and Development Program of China (Grant No. 2017YFA0302900 and 2017YFA0303103), and the Strategic Priority Research Program (B) of the Chinese Academy of Sciences (Grant No. XDB25000000). Part of the work is supported by the Synergic Extreme Condition User System. We thank the support from the Users with Excellence Program of Hefei Science Center CAS (2020HSC-UE015). JG is grateful for support from the Youth Innovation Promotion Association of the CAS (2019008).

REFERENCES

Arguilla, M. Q., Katoch, J., Krymowski, K., Cultrara, N. D., Xu, J., Xi, X., et al. (2016). $NaSn_2As_2$: An Exfoliatable Layered van der Waals Zintl Phase. *ACS Nano* 10, 9500–9508. doi:10.1021/acsnano.6b04609

Bednorz, J. G., and Muller, K. A. (1986). Possible high T_C Superconductivity in the Ba-La-Cu-O System. *Z. Phys. B - Condens. Matter* 64, 189–193. doi:10.1007/bf01303701

Cheng, E. J., Ni, J. M., Meng, F. Q., Ying, T. P., Pan, B. L., Huang, Y. Y., et al. (2018). Nodeless Superconductivity in the SnAs-based van der Waals-type Superconductor $NaSn_2As_2$. *EPL* 123, 47004. doi:10.1209/0295-5075/123/47004

Chu, C. W., Deng, L. Z., and Lv, B. (2015). Hole-doped Cuprate High Temperature Superconductors. *Phys. C: Supercond. and its Appl.* 514, 290–313. doi:10.1016/j.physc.2015.02.047

Debessai, M., Hamlin, J. J., and Schilling, J. S. (2008). Comparison of the Pressure Dependences of T_C in the Trivalent D-Electron Superconductors Sc, Y, La, and Lu up to Megabar Pressures. *Phys. Rev. B* 78, 064519. doi:10.1103/physrevb.78.064519

Gibson, Q. D., Schoop, L. M., Muechler, L., Xie, L. S., Hirschberger, M., Ong, N. P., et al. (2015). Three-dimensional Dirac Semimetals: Design Principles and Predictions of New Materials. *Phys. Rev. B* 91, 205128. doi:10.1103/physrevb.91.205128

Goto, Y., Miura, A., Moriyoshi, C., Kuroiwa, Y., Matsuda, T. D., Aoki, Y., et al. (2018). $Na_{1-x}Sn_2P_2$ as a new Member of van der Waals-type Layered tin Pnictide Superconductors. *Sci. Rep.* 8, 12852. doi:10.1038/s41598-018-31295-8

Goto, Y., Yamada, A., Matsuda, T. D., Aoki, Y., and Mizuguchi, Y. (2017). SnAs-Based Layered Superconductor $NaSn_2As_2$. *J. Phys. Soc. Jpn.* 86, 123701. doi:10.7566/jpsj.86.123701

Gui, X., Pletikosic, I., Cao, H., Tien, H.-J., Xu, X., Zhong, R., et al. (2019). A New Magnetic Topological Quantum Material Candidate by Design. *ACS Cent. Sci.* 5, 900–910. doi:10.1021/acscentsci.9b00202

Guo, J., Jin, S., Wang, G., Wang, S., Zhu, K., Zhou, T., et al. (2010). Superconductivity in the Iron selenide$K_xFe_2Se_2(0\leq x\leq 1.0)$. *Phys. Rev. B* 82, 180520 (R). doi:10.1103/physrevb.82.180520

He, B., Wang, Y., Arguilla, M. Q., Cultrara, N. D., Scudder, M. R., Goldberger, J. E., et al. (2019). The Fermi Surface Geometrical Origin of Axis-dependent Conduction Polarity in Layered Materials. *Nat. Mat.* 18, 568–572. doi:10.1038/s41563-019-0309-4

Hsu, F.-C., Luo, J.-Y., Yeh, K.-W., Chen, T.-K., Huang, T.-W., Wu, P. M., et al. (2008). Superconductivity in the PbO-type Structure α-FeSe. *Proc. Natl. Acad. Sci. U.S.A.* 105, 14262–14264. doi:10.1073/pnas.0807325105

Hu, J. P. (2016). Identifying the Genes of Unconventional High Temperature Superconductors. *Sci. Bull.* 61, 561. doi:10.1360/n972015-00702

Ishihara, K., Takenaka, T., Miao, Y., Tanaka, O., Mizukami, Y., Usui, H., et al. (2018). Evidence for s -wave Pairing with Atomic Scale Disorder in the van der Waals Superconductor $NaSn_2As_2$. *Phys. Rev. B* 98, 20503. doi:10.1103/physrevb.98.020503

Kamihara, Y., Watanabe, T., Hirano, M., and Hosono, H. (2008). Iron-Based Layered Superconductor $La[O_{1-x}F_x]FeAs$ (X = 0.05–0.12) with T_c = 26 K. *J. Am. Chem. Soc.* 130, 3296–3297. doi:10.1021/ja800073m

Kushwaha, S. K., Pletikosić, I., Liang, T., Gyenis, A., Lapidus, S. H., Tian, Y., et al. (2016). Sn-Doped $Bi_{1.1}Sb_{0.9}Te_2S$ Bulk Crystal Topological Insulator with Excellent Properties. *Nat. Commun.* 7, 11456. doi:10.1038/ncomms11456

Lee, K., Kaseman, D., Sen, S., Hung, I., Gan, Z., Gerke, B., et al. (2015). Intricate Short-Range Ordering and Strongly Anisotropic Transport Properties of Li1-xSn2+xAs2. *J. Am. Chem. Soc.* 137, 3622–3630. doi:10.1021/jacs.5b00237

Li, H., Gao, S. Y., Duan, S. F., Xu, Y. F., Zhu, K. J., Tian, S. J., et al. (2019). Dirac Surface States in Intrinsic Magnetic Topological Insulators $EuSn_2As_2$ and $MnBi_{2n}Te_{3n+1}$. *Phys. Rev. X* 9, 041039. doi:10.1103/physrevx.9.041039

Lin, Z., Wang, G., Le, C., Zhao, H., Liu, N., Hu, J., et al. (2017). Thermal Conductivities in NaSnAs, NaSnP, and$NaSn_2As_2$: Effect of Double Lone-Pair Electrons. *Phys. Rev. B* 95, 165201. doi:10.1103/physrevb.95.165201

Mao, H. K., Xu, J., and Bell, P. M. (1986). Calibration of the Ruby Pressure Gauge to 800 Kbar under Quasi-Hydrostatic Conditions. *J. Geophys. Res.* 91, 4673. doi:10.1029/jb091ib05p04673

Proust, C., and Taillefer, L. (2019). The Remarkable Underlying Ground States of Cuprate Superconductors. *Annu. Rev. Condens. Matter Phys.* 10, 409–429. doi:10.1146/annurev-conmatphys-031218-013210

Pugliese, G. M., Stramaglia, F., Goto, Y., Terashima, K., Simonelli, L., Fujiwara, H., et al. (2019). Temperature Dependent Local Atomic Displacements in $NaSn_2As_2$ System. *J. Phys. Condens. Matter* 31, 425402. doi:10.1088/1361-648x/ab2bd4

Rong, L.-Y., Ma, J.-Z., Nie, S.-M., Lin, Z.-P., Li, Z.-L., Fu, B.-B., et al. (2017). Electronic Structure of $SrSn_2As_2$ Near the Topological Critical Point. *Sci. Rep.* 7, 6133. doi:10.1038/s41598-017-05386-x

Sun, L., Chen, X.-J., Guo, J., Gao, P., Huang, Q.-Z., Wang, H., et al. (2012). Re-emerging Superconductivity at 48 Kelvin in Iron Chalcogenides. *Nature* 483, 67–69. doi:10.1038/nature10813

van der Pauw, L. J. (1958). A Method of Measuring the Resistivity and Hall Coefficient on Lamellae of Arbitrary Shape. *Philips Tech. Rev.* 20, 220.

Wang, H.-D., Dong, C.-H., Li, Z.-J., Mao, Q.-H., Zhu, S.-S., Feng, C.-M., et al. (2011). Superconductivity at 32 K and Anisotropy in $Tl_{0.58}Rb_{0.42}Fe_{1.72}Se_2$ Crystals. *EPL* 93, 47004. doi:10.1209/0295-5075/93/47004

Werthamer, N. R., Helfand, E., and Hohenberg, P. C. (1966). Temperature and Purity Dependence of the Superconducting Critical Field,H_{c2}. III. Electron Spin and Spin-Orbit Effects. *Phys. Rev.* 147, 295–302. doi:10.1103/physrev.147.295

Wu, M. K., Ashburn, J. R., Torng, C. J., Hor, P. H., Meng, R. L., Gao, L., et al. (1987). Superconductivity at 93 K in a New Mixed-phase Y-Ba-Cu-O Compound System at Ambient Pressure. *Phys. Rev. Lett.* 58, 908–910. doi:10.1103/physrevlett.58.908

Yuwen, H., Goto, Y., Jha, R., Miura, A., Moriyoshi, C., Kuroiwa, Y., et al. (2019). Enhanced Superconductivity by Na Doping in SnAs-Based Layered Compound Na1+x Sn2−x As2. *Jpn. J. Appl. Phys.* 58, 083001. doi:10.7567/1347-4065/ab2eb1

Zhao, L., Yi, C., Wang, C.-T., Chi, Z., Yin, Y., Ma, X., et al. (2021). Monoclinic $EuSn_2As_2$: A Novel High-Pressure Network Structure. *Phys. Rev. Lett.* 126, 155701. doi:10.1103/physrevlett.126.155701

Zhu, L., Wang, H., Wang, Y., Lv, J., Ma, Y., Cui, Q., et al. (2011). Substitutional Alloy of Bi and Te at High Pressure. *Phys. Rev. Lett.* 106, 145501. doi:10.1103/physrevlett.106.145501

Conflict of Interest: The authors declare that the research was conducted in the absence of any commercial or financial relationships that could be construed as a potential conflict of interest.

Publisher's Note: All claims expressed in this article are solely those of the authors and do not necessarily represent those of their affiliated organizations, or those of the publisher, the editors and the reviewers. Any product that may be evaluated in this article, or claim that may be made by its manufacturer, is not guaranteed or endorsed by the publisher.